

A Comparison between Relativistic and Semi-Relativistic Treatment in the Diquark–Quark Model[†]

M. Oettel¹ and R. Alkofer²

Institute for Theoretical Physics, Tübingen University
Auf der Morgenstelle 14, D-72076 Tübingen, Germany

Abstract

In the diquark–quark model of the nucleon including scalar and axialvector diquarks we compare solutions of the ladder Bethe–Salpeter equation in the instantaneous Salpeter approximation and in the fully covariant (i.e. four-dimensional) treatment. We obtain that the binding energy is severely underestimated in the Salpeter approximation. For the electromagnetic form factors of the nucleon we find that in both approaches the overall shapes of the respective form factors are reasonably similar up to $Q^2 \approx 0.4 \text{ GeV}^2$. However, the magnetic moments differ substantially as well as results for the pion–nucleon and the axial coupling of the nucleon.

Keywords: Bethe–Salpeter equation, Salpeter approximation, nucleon form factors

PACS: 11.10.St, 12.39.Ki, 12.40.Yx, 13.40.Gp, 14.20.Dh

[†]Supported by COSY under contract 41376610 and DFG under contract We 1254/4-1.

¹E-Mail: oettel@pion06.tphys.physik.uni-tuebingen.de

²E-Mail: reinhard.alkofer@uni-tuebingen.de

Bound states of two particles in quantum field theory can be described by solutions of integral equations such as the Bethe–Salpeter (BS) equation [1]. It has the generic form

$$\Psi(p, P) = S_1(p_1) S_2(p_2) \int \frac{d^4 p'}{(2\pi)^4} K(p, p', P) \Psi(p', P), \quad (1)$$

where S_1 and S_2 denote the fully dressed propagators of particle 1 and 2, and K is the full, 2P–irreducible interaction kernel between the in- and outgoing particles. The wave function (or Bethe–Salpeter amplitude) Ψ is not an observable quantity but it can be employed to compute e.g. form factors as matrix elements of operators [2].

Little success has been made in going beyond the ladder approximation (see, however, e.g. [3]) where the propagators S_1 and S_2 are approximated by the corresponding bare propagators and the kernel K just contains the interaction to lowest order which might be the exchange of a third particle with bare propagator S_3 :

$$\Psi(p, P) = S_1^{bare}(p_1) S_2^{bare}(p_2) \int \frac{d^4 p'}{(2\pi)^4} S_3(p, p', P) \Psi(p', P). \quad (2)$$

Even in this approximation an analytical solution to the BS equation has been found only for the Wick–Cutkosky model (for an introduction into this model see e.g. [4]). Moreover, practical attempts to solve the BS equation in various models have resorted to further approximations, especially three–dimensional reductions (for a critical comparison of different three–dimensional reductions, see [5]). The Salpeter approximation in which retardation effects in S_3 are neglected reduces the BS equation to a Klein–Gordon or Dirac equation with a hermitian Hamiltonian. It is often claimed to be covariant though the neglect of the time–component of the four–momenta p and p' seems to prohibit this phrasing. It is true, however, that the solutions obey relativistic translation invariance.

In this letter we choose a diquark–quark model of the nucleon for a comparison between the Salpeter approximation and the fully relativistic BS solution. This has two reasons: If one assumes separable diquark correlations, the three–body Faddeev equations reduce to a ladder BS equation which sums up the quark exchange between the spectator quark and the diquark quasiparticle [6, 7, 8, 9, 10, 11]. Thus the truncation of the BS kernel to the one–particle exchange is not completely arbitrary but directly linked to the separability assumption. Secondly, a comparison between relativistic and semi–relativistic solutions in the BS equations should not stop at the level of the solutions to the equations but involve observable quantities. There are several attempts to calculate observables within this framework, such as the electromagnetic form factors. This has been done in the Salpeter approximation [12, 13] and using the full solution [14, 15]. In the following we

will compare the electromagnetic form factors of the nucleon obtained in the Salpeter approximation to the ones using the full BS equation employing model parameters as in refs. [12, 13].

The diquark-quark model

The underlying approximations of the diquark–quark model are, first, the neglect of any 3–particle irreducible interactions between the quarks in the nucleon, and, secondly, the separability of correlations in the two–quark channel. The first assumption allows to derive a relativistic Faddeev equation for the 6–point quark Green’s function, and the second one reduces them to an effective quark–diquark BS equation.

The full derivation of the quark–diquark BS equation within the NJL model can be found in refs. [7, 9]. In the following we will sketch the most important steps. As usual in the treatment of the BS equation we will work in Euclidean space. Scalar and axialvector diquarks are introduced via the assumption of a separable 4–point quark function:

$$G_{\alpha\gamma,\beta\delta}^{\text{sep}}(p, q, P) := \chi_{\gamma\alpha}(p) D(P) \bar{\chi}_{\beta\delta}(q) + \chi_{\gamma\alpha}^{\mu}(p) D^{\mu\nu}(P) \bar{\chi}_{\beta\delta}^{\nu}(q) .$$

P is the total momentum of the incoming and the outgoing quark–quark pair, p and q are the relative momenta between the quarks in the two channels. $\chi_{\alpha\beta}(p)$ and $\chi_{\alpha\beta}^{\mu}(p)$ are vertex functions of quarks with a scalar and an axialvector diquark, respectively. They belong to a $\bar{3}$ –representation in color space and are either flavor antisymmetric (scalar diquark) or flavor symmetric (axialvector diquark). For their Dirac structure we will retain the dominant contribution only. Thus we introduce one scalar function $P(p)$ which depends only on the relative momentum p between the quarks,

$$\chi_{\alpha\beta}(p) = g_s(\gamma^5 C)_{\alpha\beta} P(p) , \tag{3}$$

$$\chi_{\alpha\beta}^{\mu}(p) = g_a(\gamma^{\mu} C)_{\alpha\beta} P(p). \tag{4}$$

C denotes hereby the charge conjugation matrix, and g_a and g_s are effective coupling constants obtained by normalization of the diquark states. The Pauli principle requires the relative momentum to be defined $p = \frac{1}{2}(p_{\alpha} - p_{\beta})$, where p_{α} and p_{β} are the quark momenta [15]. $P(p)$ parametrizes the extension of the vertex in momentum space. To facilitate the comparison between our work and that of [12, 13] we choose

$$P(p) = \exp(-4\lambda^2 p^2). \tag{5}$$

The propagators of scalar and axialvector diquark are the ones for a free spin-0 and spin-1 particle,

$$D(p) = -\frac{1}{p^2 + m_{sc}^2}, \quad (6)$$

$$D^{\mu\nu}(p) = -\frac{\delta^{\mu\nu} + (1 - \xi)\frac{p^\mu p^\nu}{m_{ax}^2}}{p^2 + m_{ax}^2}. \quad (7)$$

ξ is a gauge parameter introduced in [16], and in the following we will put $\xi = 1$. The constituent quark propagator is simply the free fermion propagator

$$S(p) = \frac{i\not{p} - m_q}{p^2 + m_q^2}. \quad (8)$$

The nucleon BS wave function can be described by an effective multi-spinor characterizing the scalar and axialvector correlations (see e.g. [11]),

$$\Psi(p, P)u(P) = \begin{pmatrix} \Psi^5(p, P) \\ \Psi^\mu(p, P) \end{pmatrix} u(P) \quad (9)$$

where $u(P)$ is a positive-energy Dirac spinor with P being the total momentum of the bound state. p is the relative momentum between quark and diquark, respectively. The vertex function is defined by amputating the legs off the wave function,

$$\begin{pmatrix} \Phi^5 \\ \Phi^\mu \end{pmatrix} = S^{-1} \begin{pmatrix} D^{-1} & 0 \\ 0 & (D^{\mu\nu})^{-1} \end{pmatrix} \begin{pmatrix} \Psi^5 \\ \Psi^\nu \end{pmatrix}. \quad (10)$$

The BS equation is a system of equations for wave and vertex function that takes the compact form

$$\int \frac{d^4 p'}{(2\pi)^4} G(p, p', P) \begin{pmatrix} \Psi^5 \\ \Psi^{\mu'} \end{pmatrix} (p', P) = 0 \quad (11)$$

where the object $G(p, p', P)$ involves the propagators of quark and diquark and the interaction kernel that describes the quark exchange between quark and diquark,

$$G(p, p', P) = (2\pi)^4 \delta(p - p') S^{-1}(p_q) \begin{pmatrix} D^{-1} & 0 \\ 0 & (D^{\mu'\mu})^{-1} \end{pmatrix} (p_d) + \frac{1}{2} \begin{pmatrix} \chi S^T(q) \bar{\chi} & -\sqrt{3} \chi^{\mu'} S^T(q) \bar{\chi} \\ -\sqrt{3} \chi S^T(q) \bar{\chi}^\mu & -\chi^{\mu'} S^T(q) \bar{\chi}^\mu \end{pmatrix}. \quad (12)$$

The partitioning of the momentum between quark and diquark introduces a parameter η with $p_q = \eta P + p$ and $p_d = (1 - \eta)P - p$. Therefore the momentum of the exchanged quark is $q = -p - p' + (1 - 2\eta)P$. The relative momentum of the quarks at the diquark vertex χ is $p_2 = p + p'/2 - (1 - 3\eta)P/2$ and the one at the conjugated vertex $\bar{\chi}$ is

$p_1 = p/2 + p' - (1 - 3\eta)P/2$. Relativistic translation invariance requires that if $\Phi(p, P; \eta_1)$ is a solution of the BS equation then also $\Phi(p + (\eta_2 - \eta_1)P, P; \eta_2)$ is one.

The BS equation (11) is solved in the rest frame of the bound state, $P = \begin{pmatrix} \mathbf{0} \\ iM \end{pmatrix}$. In this frame the Salpeter approximation amounts to neglecting the fourth component of all vectors appearing in the interaction, *i.e.* of the vectors q , p_1 and p_2 . The immediate consequence is that the vertex function will depend only on the relative three-momentum, $\Phi(p, P) \equiv \Phi(\vec{p})$.

Numerical Solutions

In the following we use the complete partial wave decomposition of wave and vertex function for octet baryons given in [11],

$$\begin{pmatrix} \Phi^5(p, P) \\ \Phi^4(p, P) \\ \Phi(p, P) \end{pmatrix} = \begin{pmatrix} \begin{pmatrix} \mathbf{1} S_1 & 0 \\ \frac{1}{p}(\boldsymbol{\sigma}\mathbf{p}) S_2 & 0 \\ \frac{1}{p}(\boldsymbol{\sigma}\mathbf{p}) A_1 & 0 \\ \mathbf{1} A_2 & 0 \end{pmatrix} \\ \begin{pmatrix} i\hat{\mathbf{p}}(\boldsymbol{\sigma}\hat{\mathbf{p}})A_3 + (\boldsymbol{\sigma} \times \hat{\mathbf{p}})(\boldsymbol{\sigma}\hat{\mathbf{p}})A_5 & 0 \\ \frac{i}{p}\mathbf{p}A_4 + \frac{1}{p}(\boldsymbol{\sigma} \times \mathbf{p})A_6 & 0 \end{pmatrix} \end{pmatrix}. \quad (13)$$

The unknown scalar functions S_i and A_i are functions of $p^2 = p^\mu p^\mu$ and of the angular variable $z = \hat{P} \cdot \hat{p}$ which denotes the cosine of the angle between p^μ and the 4-axis. As explained above, the functional dependence collapses in the Salpeter approximation from the two variables (p^2, z) to the single variable $p^2(1 - z^2)$. We expand the scalar functions in terms of Chebyshev polynomials of the first kind in the variable z ,

$$S_i[A_i](p^2, z) = \sum_{n=0}^{\infty} i^n S_i^n[A_i^n](p^2) T_n(z), \quad (14)$$

and derive a system of coupled integral equations for the Chebyshev momenta $S_i^n[A_i^n]$ that we solve iteratively as described in [11, 15]. This expansion is very close to the hyperspherical expansion that has been shown to work extraordinarily well in the massive Wick–Cutkosky model [17, 18] and in quenched QED [18]. This finding has been corroborated by [11] in the diquark–quark model for pointlike diquarks.

As stated already we adopt the parameters of refs. [12, 13]. In the case of the scalar–axialvector diquark model this especially includes identical diquark normalizations leading to equal diquark–quark–quark couplings in the scalar and axialvector channel, $g_s = g_a$. The BS equation (11) can be written as an eigenvalue problem for g_s . This coupling is adjusted to yield the physical nucleon mass $M=0.939$ GeV for given values of the

Set		m_q [GeV]	m_{sc} [GeV]	m_{ax} [GeV]	λ [fm]	g_s
I	Salpeter full	0.35	0.65	-	0.18	20.0 (20.0) 16.5
II	Salpeter full	0.35	0.65	0.65	0.24	12.3 (11.5) 9.6

Table 1: The two parameter sets of the model.

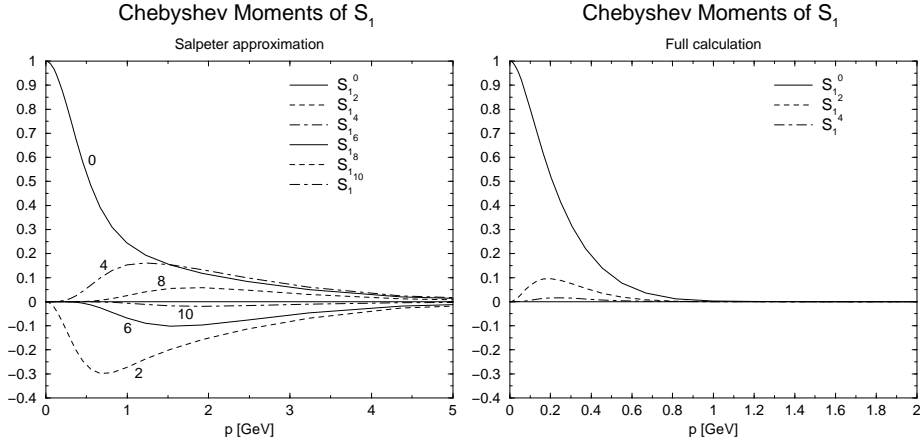


Figure 1: The Chebyshev expansion of the dominant scalar function $S_1(p, z)$ in the Salpeter approximation and the full calculation.

quark and diquark mass as well as the diquark width λ . In table 1 we have listed the two sets of parameters, scalar diquark only and scalar–axialvector diquark model, with their corresponding eigenvalues obtained by us in the full calculation and the Salpeter approximation. The values in parentheses are the ones from refs. [12, 13]. Please note that due to a different flavor normalization these values had to be multiplied by $\sqrt{2}$ to be directly comparable to ours.

Although we could reproduce the eigenvalue for the model case with scalar diquark only, this is not the case for Set II. We observe that the calculations of [13] involved only 4 instead of 6 axialvector components of Φ^μ , namely the projected ones onto zero orbital angular momentum and the corresponding lower components. Still one would expect a higher eigenvalue in the reduced system. *The more striking observation is the amplification of the eigenvalue by about 20...25% in the Salpeter approximation although the binding energy is small, being only 6% of the sum of the constituent masses.*

The substantial difference between the two approaches is also reflected in the vertex function solutions themselves. Fig. 1 shows the Chebyshev moments of the dominant

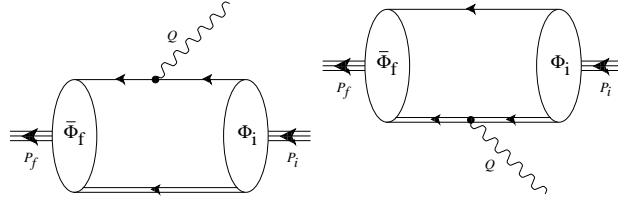


Figure 2: Impulse approximation diagrams contributing to the electromagnetic current.

scalar function S_1 for both methods using the parameters of Set I. Only the even momenta are given, since the odd ones are zero in the Salpeter approximation (but are present, of course, in the full calculation). Two things are manifest: The Salpeter amplitudes have a much broader spatial extent than the full amplitudes. Secondly, the expansion in Chebyshev polynomials that relies on an approximate $O(4)$ symmetry converges much more rapidly for the full solution but is hardly convincing in the Salpeter approximation. Again, since the scalar functions depend in the Salpeter approximation on just one variable, $p^2(1-z^2)$, our expansion is a cumbersome way of visualizing the solution but makes clear that the Salpeter approximation strongly violates the $O(4)$ -symmetry.

Electromagnetic Form Factors

The Sachs form factors G_E and G_M can be extracted from the solutions of the BS equations using the relations

$$G_E = \frac{M}{2P^2} \text{Tr} \langle J^\mu \rangle P^\mu, \quad G_M = \frac{iM^2}{Q^2} \text{Tr} \langle J^\mu \rangle \gamma_T^\mu, \quad (15)$$

$$\langle J^\mu \rangle = \int \frac{d^4 p_f}{(2\pi)^4} \int \frac{d^4 p_i}{(2\pi)^4} \bar{\Phi}^T(P_f, p_f) J^\mu \Phi(P_i, p_i). \quad (16)$$

with the definitions $P = (P_i + P_f)/2$ and $\gamma_T^\mu = \gamma^\mu - \hat{P}^\mu \not{P}$. To this end, one has to normalize the wave and the vertex function through the condition

$$- \int \frac{d^4 p}{(2\pi)^4} \int \frac{d^4 p'}{(2\pi)^4} \bar{\Psi}(p', P_n) \left[P^\mu \frac{\partial}{\partial P^\mu} G(p', p, P) \right]_{P=P_n} \Psi(p, P_n) \stackrel{!}{=} M \Lambda^+ \quad (17)$$

which uses the definition of G given in eq. (12) and employs the positive-energy projector Λ^+ . This normalization integral is again performed easily in the rest frame of the bound state, additionally the double integral over the interaction kernel drops out in the Salpeter approximation since the kernel is independent of P .

The current operator J^μ in eq. (16) contains all possible couplings of the photon to the kernel G of the BS equation. The two simplest contributions make up the impulse approximation pictorially shown in Fig. 2. Since the impulse approximation does not mix

scalar and axialvector amplitudes there are altogether four diagrams to compute: quark and diquark coupling and for each of the two the matrix element between scalar and axialvector amplitudes of the nucleon. Flavor algebra [13] yields the following current matrix elements for proton and neutron,

$$\langle J_{proton}^\mu \rangle = \frac{2}{3}\langle J_{q,s}^\mu \rangle + \frac{1}{3}\langle J_{dq,s}^\mu \rangle + \langle J_{dq,a}^\mu \rangle, \quad (18)$$

$$\langle J_{neutron}^\mu \rangle = -\frac{1}{3}\langle J_{q,s}^\mu \rangle + \frac{1}{3}\langle J_{dq,s}^\mu \rangle + \frac{1}{3}\langle J_{q,a}^\mu \rangle - \frac{1}{3}\langle J_{dq,a}^\mu \rangle. \quad (19)$$

The Salpeter approximation enjoys the nice property that the nucleon current is conserved at the level of the impulse approximation. Furthermore there is the peculiar identity at zero photon momentum transfer,

$$\langle J_{q,s[a]}^\mu(Q^2 = 0) \rangle = \langle J_{dq,s[a]}^\mu(Q^2 = 0) \rangle \quad (20)$$

which guarantees that proton and neutron have their correct charge (i.e. $G_E^p(Q^2 = 0) = 1$, $G_E^n(Q^2=0)=0$). This is *not* so in the full calculation, to ensure current conservation and the physical charges one has to take into account all diagrams of the photon coupling to the interaction part of G . These diagrams are shown in fig. 3, the proof of this assertion and the construction of the "seagull" diagrams (photon coupling to the diquark-quark vertices) can be found in [15], see also [19] for a general discussion of the current operator in three-body theory.

In fig. 4 the electric form factors of proton and neutron are displayed, using parameter set II. The first observation is that in the Salpeter approximation we could not obtain convergence with the expansion in Chebyshev polynomials beyond $Q^2 \approx 0.4 \text{ GeV}^2$. We computed the form factors in the Breit frame where Q is real but $z_i = \hat{p}_i \cdot \hat{P}_i$ and $z_f = \hat{p}_f \cdot \hat{P}_f$ have imaginary parts and their absolute values may exceed one, except for the case of no momentum transfer [11]. So this expansion that works in the rest frame, and it does barely so for the Salpeter approximation, will not generally work in a moving frame. On the other hand, the decrease of the higher Chebyshev moments is so drastic for the full

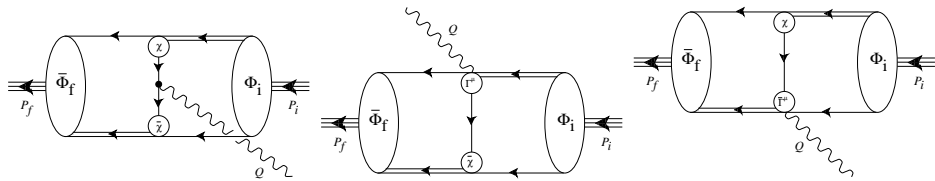


Figure 3: Exchange diagrams contributing to the electromagnetic current.

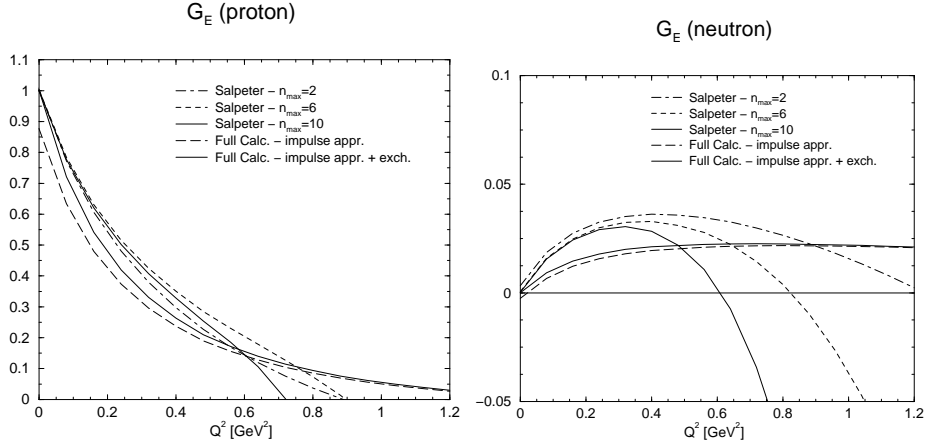


Figure 4: Nucleon electric form factors in the Salpeter approximation and in the full calculation. The curves for the Salpeter approximation have been obtained by including the Chebyshev moments of the vertex function up to order n_{max} .

four-dimensional solution that form factor calculations converge easily up to several GeV^2 [15, 20]. However, as can be seen from fig. 4 the Salpeter approximation badly fails above 0.5 GeV^2 thereby revealing its semi-relativistic nature.

The second finding concerns the electromagnetic radii. The Salpeter approximation tends to underestimate the proton charge radius and to overestimate the absolute value of the neutron charge radius, see the first two rows of table 3. The axialvectors tend to suppress the neutron electric form factor much more in the full calculation than in the Salpeter approximation.

Turning to the magnetic moments, the contributions of the various diagrams are tabulated in table 2 for the proton. Following [13] we ascribed to the axialvector diquark a rather large anomalous magnetic moment of $\kappa=1.6$ which was needed by the cited author to fit the proton magnetic moment. As already observed earlier, we could reproduce the magnetic moment for Set I, however, for Set II, the values differ and especially the cou-

Set		$\mu_{sc,q}$	$\mu_{sc,dq}$	$\mu_{ax,q}$	$\mu_{ax,dq}$	μ_{ex}	SUM
I	Salpeter	1.57	0.01	-	-	-	1.58 (1.58)
	full	2.04	0.01	-	-	0.33	2.38
II	Salpeter	0.92 (1.08)	0.00	0	1.37 (1.7)	-	2.29 (2.78)
	full	1.09	0.00	0	0.98	0.38	2.45

Table 2: Contributions to the proton magnetic moment from the single diagrams. The first index refers to the nucleon amplitudes involved and the second to the photon coupling to either quark or diquark. In parentheses the values of refs. [12, 13] are given.

Set		$(r_p)_{\text{el}}$ [fm]	$(r_n^2)_{\text{el}}$ [fm ²]	μ_p	$(r_p)_{\text{mg}}$ [fm]	μ_n	$(r_n)_{\text{mg}}$ [fm]	$g_{\pi NN}$	$r_{\pi NN}$ [fm]	g_A	r_A [fm]
I	Salp.	0.89	-0.28	1.58	1.04	-0.77	1.05	8.96	1.04	0.93	0.93
	full	0.99	-0.23	2.38	1.06	-1.65	1.00	15.34	1.04	1.46	1.02
II	Salp.	0.88	-0.06	2.29	0.85	-0.98	0.94	6.03	1.15	0.53	1.08
	full	1.01	-0.04	2.45	0.99	-1.26	1.05	9.36	1.15	0.82	1.10

Table 3: Some static quantities of the nucleon.

pling to the axialvector diquark is much weaker in our Salpeter calculation. Rather more interesting is the comparison in the full calculation between Set I and Set II: The axialvector diquark improves the magnetic moment only marginally! The Salpeter approximation tends to overestimate this contribution quite drastically.

Finally we want to mention that the Salpeter approximation underestimates the pion–nucleon coupling $g_{\pi NN}$ and the axial coupling g_A quite sizeably, see table 3.

Conclusions

In this letter we have presented results for a covariant diquark–quark model. The ladder BS equation for the nucleon has been solved in a fully covariant way and in the instantaneous Salpeter approximation. As for the model with scalar diquarks only we have verified the results of ref. [12] whereas there are discrepancies if the axialvector diquark is included. Part of these differences are due to the fact that in ref. [13] not all (ground state) axialvector components have been taken into account. Additionally, we take our result as an indication that the calculations presented in ref. [13] might suffer from some minor error.

The main purpose of this letter is the comparison of observables calculated in the Salpeter approximation to the ones obtained in the fully four–dimensional scheme. The first very surprising observation is the overestimation of the BS eigenvalue in the Salpeter approximation. Phrased otherwise, for a given coupling constant the binding energy would be much too small in the Salpeter approximation. We have also demonstrated that the Salpeter approximation violates badly the approximate O(4) symmetry of the BS equation. This has drastic consequences for the resulting nucleon electromagnetic form factors if the photon virtuality exceeds 0.4 GeV². Whereas different nucleon radii differ only mildly in these two approaches one sees very clearly that the results for the magnetic moments, the pion–nucleon coupling and the axial coupling are underestimated drastically in the Salpeter approximation.

Acknowledgement

We thank S. Ahlig, H. Reinhardt and H. Weigel for a critical reading of the manuscript and their comments.

References

- [1] E. E. Salpeter and H. A. Bethe, Phys. Rev. **84** (1951) 1232.
- [2] S. Mandelstam, Proc. Roy. Soc. **233** (1955) 248.
- [3] L. Theussl and B. Desplanques, nucl-th/9908007.
- [4] Z.K. Silagadze, hep-ph/9803307.
- [5] J. Bijtebier, Nucl. Phys. **A623** (1997) 498.
- [6] R. T. Cahill, Austr. J. Phys. **42** 171 (1989) 171.
- [7] H. Reinhardt, Phys. Lett. **B244**, (1990) 316.
- [8] A. Buck, R. Alkofer, and H. Reinhardt, Phys. Lett. **B286** (1992) 29.
- [9] N. Ishii, W. Bentz and K. Yazaki, Nucl. Phys. **A587** (1995) 617.
- [10] K. Kusaka, G. Piller, A. W. Thomas and A. G. Williams, Phys. Rev. **D55** (1997) 5299.
- [11] M. Oettel, G. Hellstern, R. Alkofer and H. Reinhardt, Phys. Rev. **C58** (1998) 2459.
- [12] V. Keiner, Z. Phys. **A354** (1996) 87.
- [13] V. Keiner, Phys. Rev. **C54** (1996) 3232.
- [14] G. Hellstern, R. Alkofer, M. Oettel and H. Reinhardt, Nucl. Phys. **A627** (1997) 679.
- [15] M. Oettel, M.A. Pichowsky and L. von Smekal, nucl-th/9909082.
- [16] T.D. Lee and C.N. Yang, Phys. Rev. **128** (1962) 885.
- [17] T. Nieuwenhuis and J.A. Tjon, Few Body Syst. **21** (1996) 167.
- [18] S. Ahlig and R. Alkofer, Ann. Phys. **275** (1999) 113.
- [19] A.N. Kvinikhidze and B. Blankleider, Phys. Rev. **C 60** (1999) 044003; 044004.
- [20] J. C. R. Bloch, C. D. Roberts, S. M. Schmidt, A. Bender and M.R. Frank, Phys. Rev. **C60** (1999) 062201; J. C. R. Bloch, C. D. Roberts, S. M. Schmidt, nucl-th/9911068.